Shock compression of condensed matter using intense beams of energetic heavy ions

N. A. Tahir,[1] D. H. H. Hoffmann,[1,2] A. Kozyreva,[2] A. Shutov,[3] J. A. Maruhn,[4] U. Neuner,[2] A. Tauschwitz,[2] P. Spiller,[2] and R. Bock[2]

[1]*Institut für Kernphysik, Technische Universität Darmstadt, Schlossgarten Strasse 9, 64289 Darmstadt, Germany*

[2]*Gesellschaft für Schwerionenforschung, Planckstrasse 1, 64291 Darmstadt, Germany*

[3]*Institute for Chemical Physics Research, Chernogolovka, Russia*

[4]*Institut für Theoretische Physik, Universität Frankfurt, Postfach 11 19 32, 60054 Frankfurt, Germany*

(Received 28 July 1999; revised manuscript received 5 October 1999)

In this paper is presented, with the help of sophisticated two-dimensional hydrodynamic simulations, a suitable design with optimized parameters for a heavy-ion beam-matter interaction experiment that will be carried out at the Gesellschaft für Schwerionenforschung (GSI) Darmstadt by the end of the year 2001 when the upgrade of the existing accelerator facility will be completed. Our simulations show that this upgraded heavy-ion beam is capable of generating strong shocks in solid targets that compress the target material to supersolid densities and generate multi-mbar pressures. This will open up, at the GSI, the possibility of investigation of the equation-of-state properties of matter under such extreme conditions. Numerical simulations can predict the experimental results with reasonable accuracy, which is helpful in designing the diagnostic tools for the experiment.

PACS number(s): 51.50.+v, 25.75.−q, 62.50.+p, 79.20.Rf

I. INTRODUCTION

Due to high accelerator efficiency, high repetition rate, and favorable energy deposition behavior of heavy ions in matter [1–10], it is expected that a heavy-ion driver would be the best tool by which to operate any future inertial confinement fusion (ICF) power plant. Moreover, intense beams of energetic heavy ions are excellent tools for generating strongly coupled, high-density plasmas [11–13]. These plasmas are of great interest in astrophysics because it is known that the interiors of giant planets and stars are made of such matter. Exact knowledge of equation-of-state (EOS) properties of matter under such extreme conditions (supersolid density and multimegabar pressures) based on careful experimental studies is therefore very important in order to understand planetary as well as stellar structure and to advance our knowledge about the formation and evolution of the universe. In addition to that, there are a number of potential industrial applications for this field, including the possibility of creating metallic hydrogen in the laboratory [14–17].

During the past few decades, sophisticated theoretical models have been developed to evaluate the EOS parameters of matter. Using these theoretical models, extensive EOS data tables that cover wide ranges of density, temperature, and pressure have been generated. A typical example is the Los Alamos equation-of-state data library, SESAME that is very widely used by the scientific community. However, due to the complexity of these models, it is not possible to judge the accuracy of this data, especially in the high-density, high-temperature regime. With the development of high-power lasers, it has become possible to induce very high energy density in matter and study the EOS properties of such samples in the pressure, density, and temperature ranges that were not previously accessible by other means. Several important experiments have been done in this field using the existing laser systems [18–20] and pressures of the order of tens of mbar have been generated. This work has shown that in certain cases, significant deviations exist between the experimental results and the SESAME data. It is therefore very important to check the validity of the theoretical models over the entire range of the physical parameters of interest.

Intense beams of energetic heavy ions offer an additional tool with which to investigate the equation-of-state properties of matter under extreme conditions. Heavy ions have a number of advantages over lasers, as described below. Laser light penetrates up to the critical density surface and from that region the energy is carried to the ablation surface by a number of transport processes including electron thermal conductivity, superthermal electron transport, and radiation transport. The ablating material generates an ablation pressure that drives shock waves into the overdense region. A small fraction of the laser energy is used in the generation of these shock waves, while the bulk of the energy resides in the corona. Moreover, in laser-heated targets, creation of fast electrons is always a serious possibility. If the production of these nonthermal electrons is not properly suppressed, they may preheat the material, which will weaken the shock wave. The spot radius of the laser beam is very small (of the order of 100 μm), which makes the dimensions of the material sample under consideration very small. In addition, the time duration of the laser pulse is of the order of a few ns, which makes the lifetime of the plasma and hence the time available for experimental investigations very short.

Heavy ions, on the other hand, penetrate deep into the target material and deposit their energy in solid matter along their trajectory. The penetration depth of these ions is primarily determined by the initial ion energy and the physical state of the target material. Heavy ions are therefore capable of generating extended volumes of solid density plasmas. Unlike lasers, all of the heavy-ion beam energy is deposited in the high-density material and this energy is used to generate the shock waves in the target. Another property that is unique to the heavy-ion-beam method of inducing high en-

ergy density in matter is the fact that the amount of energy that is deposited inside the large volume of the target can be measured with high precision. This can be achieved by measuring the energy loss of the beam and the total number of ions traversing the target. In the case of laser-produced plasmas, this may not be possible. Since the specific energy deposition is almost uniform along most of the particle trajectory (except in the Bragg peak and neighboring region), there are no sharp gradients of density, temperature, and pressure in an ion-beam-heated target, which is not the case in a laser-heated target. Such a system is much more attractive for experimental studies compared to the laser-heated targets, where sharp gradients of the above physical parameters exist between the absorption region and the ablation front. Moreover, unlike the lasers, heavy ions do not generate any fast electrons and preheating by these fast electrons is not a problem in this case. In addition, the time scale of evolution of heavy-ion-beam-generated plasmas is of the order of a few hundred ns, which provides a longer time for experimental studies.

To summarize, ion-beam plasmas offer much greater homogeneity, no sharp gradients, and much longer time scales compared to the laser-produced plasmas.

The heavy-ion synchrotron (SIS) at the Gesellschaft für Schwerionenforschung (GSI), Darmstadt is a unique facility that can deliver high-intensity heavy-ion beams over a wide range of parameters. Planned future developments [21,22] will further improve the beam intensity significantly. It is expected that after the completion of the current SIS upgrade, which includes introduction of a new high-current injector and a powerful rf buncher, the SIS will be able to accelerate an intense beam of U^{+28} ions to a particle energy of 200 MeV/u. Employment of a multiturn injection scheme will allow one to accelerate about 2×10^{11} particles in the beam that will be delivered in about 50 ns. The total beam energy will be of the order of 1.5 kJ. It is expected that this upgrade will be completed by the end of the year 2001.

Numerical simulations show that these beam parameters would lead to temperatures of about 10 eV and pressures of a few mbar in solid matter. This temperature regime is therefore dominated by pure hydrodynamic effects. It should thus be possible to generate strong shocks in appropriately designed heavy-ion-beam heated solid targets that would lead to a high-density, high-pressure regime that is interesting for equation-of-state measurements of different materials.

Previously [23,24], we proposed a beam-target geometry in which we considered a solid cylindrical target and the beam was incident on one face of this cylinder. The length of the cylinder was assumed to be less than the penetration depth of the ions. In such a case the ion beam deposits a part of its energy in the target and emerges from the opposite face of the cylinder with reduced energy. Since the Bragg peak lies outside the target, the energy deposition in the target along the particle trajectory is fairly uniform. We also assumed that the beam radius was less than the target radius and that therefore the central part of the target that lies within the beam radius was strongly heated by the beam. This cylinder of heated material is surrounded by a thick cylindrical shell of solid cold matter. The pressure in the hot zone increases substantially, and that launches a shock wave into the surrounding cold part of the target, thereby compressing and heating the material. Our simulations showed that if the length of the cylinder of the heated material was made a few times larger than its radius, one could neglect the hydrodynamic expansion of the target along the cylinder length over the time scale of our interest (a few hundred ns). In such a case, therefore, the problem is reduced to that of one-dimensional shock wave propagation along the cylinder radius and one may use a one-dimensional computer program to simulate this experiment. For this reason we employed a one-dimensional, Lagrangian, hydrodynamic computer model, MEDUSA-KAT [25] to simulate the hydrodynamic response of such ''subrange'' targets made of different materials, including lead, aluminum, frozen neon, and frozen hydrogen, that were irradiated by the future SIS beam.

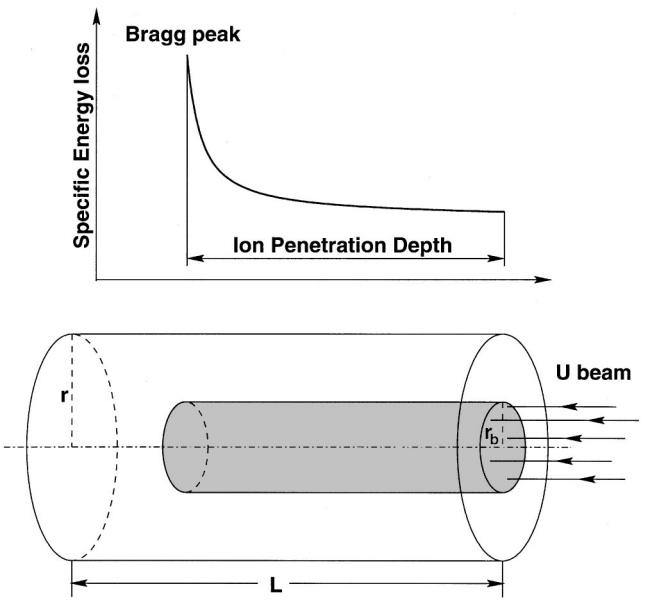

FIG. 1. Beam-target geometry for shock wave experiments at the GSI heavy-ion synchrotron facility.

Although the above beam-target arrangement simplifies the problem substantially, a significant portion of the ion-beam energy is not made use of and the specific energy deposition in the target remains low, about 50 kJ/g. In order to make use of all the beam energy, one should design ''super-range'' targets, which means that the target length is chosen to be larger than the penetration depth of the projectile ions. In such a configuration, the Bragg peak lies inside the target (as shown in Fig. 1) and the energy deposition in the target along the particle trajectory is not uniform, being about a factor of 2 higher in the Bragg peak region compared to the rest of the irradiated target regions. As a consequence, the pressure in the heated region is much higher in the Bragg peak region, which would launch a much stronger shock wave as compared to that in case of ''subrange'' targets [23,24]. This would lead to a much stronger compression of the target and much higher pressures would be generated in the shock-compressed region. Since the pressure profile in the beam-heated region in this case is not uniform, the corresponding shock wave that will be generated by this pressure profile will no longer be a one-dimensional problem. One would require a two-dimensional hydrodynamic model to simulate such an experiment.

We have employed a two-dimensional hydrodynamic computer code called BIG2 [26] to carry out numerical simulations of the hydrodynamic response of this ''super-range'' target that is irradiated by the future SIS beam. In Sec. II we present the target and beam parameters, while the simulation results are discussed in Sec. III. The conclusions drawn from this work are noted in Sec. IV.

II. TARGET AND BEAM PARAMETERS

The specific power deposition by the ion beam into the target material is an important parameter, as it determines the final temperature that could be achieved in the target. This parameter is defined by

$$P_s = \frac{E_s}{\tau}, \tag{1}$$

where τ is the pulse duration and E_s is the specific energy deposition given by

$$E_1 = \frac{\frac{1}{\rho}\frac{dE}{dx}N}{\pi r_b^2}. \tag{2}$$

In the above equation, $(1/\rho)(dE/dx)$ is the specific energy loss of a single ion, ρ is the target material density, x is the coordinate along the particle trajectory, N is the total number of particles in the beam, and r_b is the beam radius.

The beam target geometry proposed herein for experiments is shown in Fig. 1. The target considered in the calculations is a solid lead cylinder with a length $L=4$ mm and a radius $r=3$ mm. The right face of this cylinder is irradiated by 2×10^{11} particles of uranium with an energy of 200 MeV/u. It is expected that these beam parameters will be available at the GSI accelerator facility by the end of the year 2001. The beam power deposition profile along the target radius, considered to be Gaussian, is given by

$$P(r) = P_0 \exp\left[-\frac{r^2}{2\sigma^2}\right], \tag{3}$$

where σ is the standard deviation of the Gaussian distribution.

As shown by Eq. (2), the specific energy deposited in the target and hence the maximum achievable temperature and pressure are fairly strong functions of the beam radius r_b. Since 1991, GSI has employed a quadrupole final focusing system that consists of five quadrupole magnets that focus the heavy-ion beam onto a spot having a radius of 450 μm [27–29]. In order to minimize beam losses that occur at high transverse emittances, an additional plasma lens was developed and installed after the quadrupole system [30]. As mentioned before, the future SIS beam will have a much shorter pulse length of 50 ns compared to that of 300 ns which is currently available. Due to this strong pulse compression, the momentum spread will grow to about 1%. As a consequence, strong chromatic aberrations, especially those of the second order, are expected to occur. Detailed ion-optics calculations, including the transport system from the SIS to the target, show that the beam spot radius in this case would be about 1 mm [31].

In the calculations presented in this paper, we therefore assume a full width at half maximum (FWHM) of 1 mm for the Gaussian distribution represented by Eq. (3), which may be regarded as the effective beam radius.

The time profile of the beam power, assumed to be parabolic, is given by

$$P(t) = -\frac{6E}{\tau^3}[t^2 - \tau t], \tag{4}$$

where E is the total energy in the beam and in this case is about 1.5×10^3 J. The duration of the pulse τ is assumed to be 50 ns.

III. NUMERICAL SIMULATION RESULTS

The purpose of the simulations presented in this section is to propose the design and suitable target parameters that are optimized with respect to the beam parameters for a heavy-ion-matter interaction experiment to generate strong shock waves in solid matter. The shock waves will lead to high target compression and would generate multi-mbar pressures, which will make it possible to investigate the EOS properties of matter under such extreme conditions in the laboratory. Such experiments will be carried out at the GSI Darmstadt accelerator facility after the upgraded SIS beam is available by the end of the year 2001. Moreover, these simulations can predict the results of future experiments with a reasonable accuracy that may be helpful in designing the diagnostic tools needed to analyze the experiments. These simulations have been carried out using a one-temperature, two-dimensional hydrodynamic computer code BIG2 [26]. This code is based on the Godunov numerical scheme and has a second-order accuracy in space in solving hydrodynamic equations. It uses a rectangular grid and it includes electron thermal conductivity and a sophisticated equation of state described elsewhere [12,32]. It also includes energy deposition by the projectile ions taking into account the beam geometry.

In order to evaluate the specific power deposition in the target material one needs to substitute the $(1/\rho)(dE/dx)$ term in Eq. (2). We evaluate this term using the energy deposition code TRIM [33] that provides the energy loss of the incident ions in cold matter. This is a very reasonable approximation because with the above beam parameters one can only achieve a target temperature of the order of 10 eV [23,24]. At higher temperatures when the target material becomes ionized, one must take into account the enhanced stopping due to the free electrons.

As shown in Fig. 1, the heavy-ion beam is incident on the right face of the cylindrical target and the ions penetrate along the cylinder length, depositing their energy along this trajectory. In Fig. 2 we plot the specific energy deposition E_s along the target length at two values of radius r, namely, 0.0 mm and 0.5 mm at $t=50$ ns when the pulse has delivered its total energy. It is seen that starting from the right face, the ions penetrate the target up to about 1.7 mm, which according to the TRIM code is the range of 200-MeV uranium ions

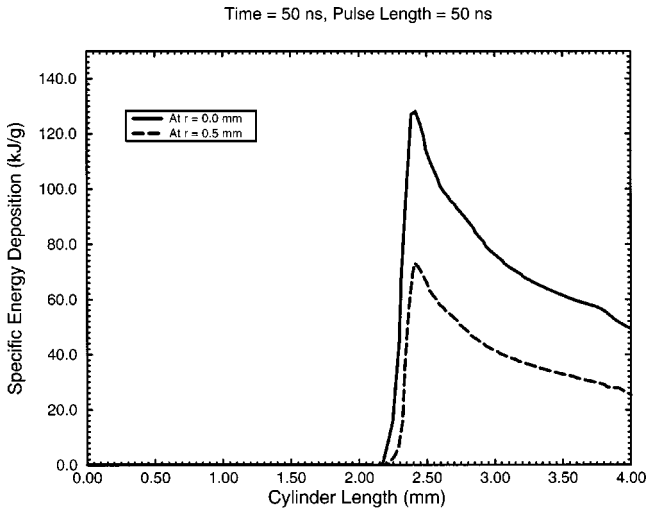

FIG. 2. Specific energy deposition along target length at $r=0.0$ mm and 0.5 mm at $t=50$ ns (time when the beam has delivered its total energy).

in solid cold lead. The Bragg peak therefore lies at $L=2.3$ mm, which is 1.7 mm to the left of the right face of the target. It is also seen from Fig. 2 that the curve corresponding to $r=0.0$ mm shows a much higher value of E_s than that for $r=0.5$ mm. This is because of the Gaussian nature of the beam deposition along the radius. Moreover, it is seen that a maximum value of E_s of about 130 kJ/g is achieved at $r=0.0$ mm (maximum of the Gaussian) and $L=2.3$ mm (Bragg peak region).

The total beam energy is delivered at $t=50$ ns and in Figs. 3(a), 3(b), and 3(c), respectively we plot the target density, temperature, and pressure at this time on a length-radius plane. It is seen that the temperature is the highest in the Bragg peak region and is of the order of 13 eV. Moreover, due to the Gaussian profile of the power deposition in the radial direction, there is a corresponding behavior of the temperature along the target radius.

Figure 3(a) shows that a shock wave has started to develop ahead of the Bragg peak region and the maximum density in the shock-compressed region is about 22 g/cm^3, which is almost twice the solid lead density (11.34 g/cm^3). It is also interesting to note that due to the combined effect of the Bragg peak and a Gaussian power deposition along the radius, the development of the shock wave along the cylinder axis is faster than that in the radial direction. The density in the Bragg peak region is below solid lead density. The pressure exhibits double peak behavior, as indicated by Fig. 3(c), which is a very interesting feature and is due to the following reason. In the shock-compressed region, the density is about 22 g/cm^3, while the temperature is relatively low (of the order of 1 eV) and the corresponding pressure is about 3 Mbar, which leads to the smaller pressure peak. This region therefore represents a high pressure and high density but low-temperature regime, which is the regime of nonideal plasmas. In the Bragg peak region, on the other hand, although the temperature is very high (about 13 eV), the pressure is relatively low (of the order of 2.5 Mbar) because the density is well below the solid density. This region therefore belongs to that state of matter has high temperature, low density, and relatively low pressure. On the right-hand side

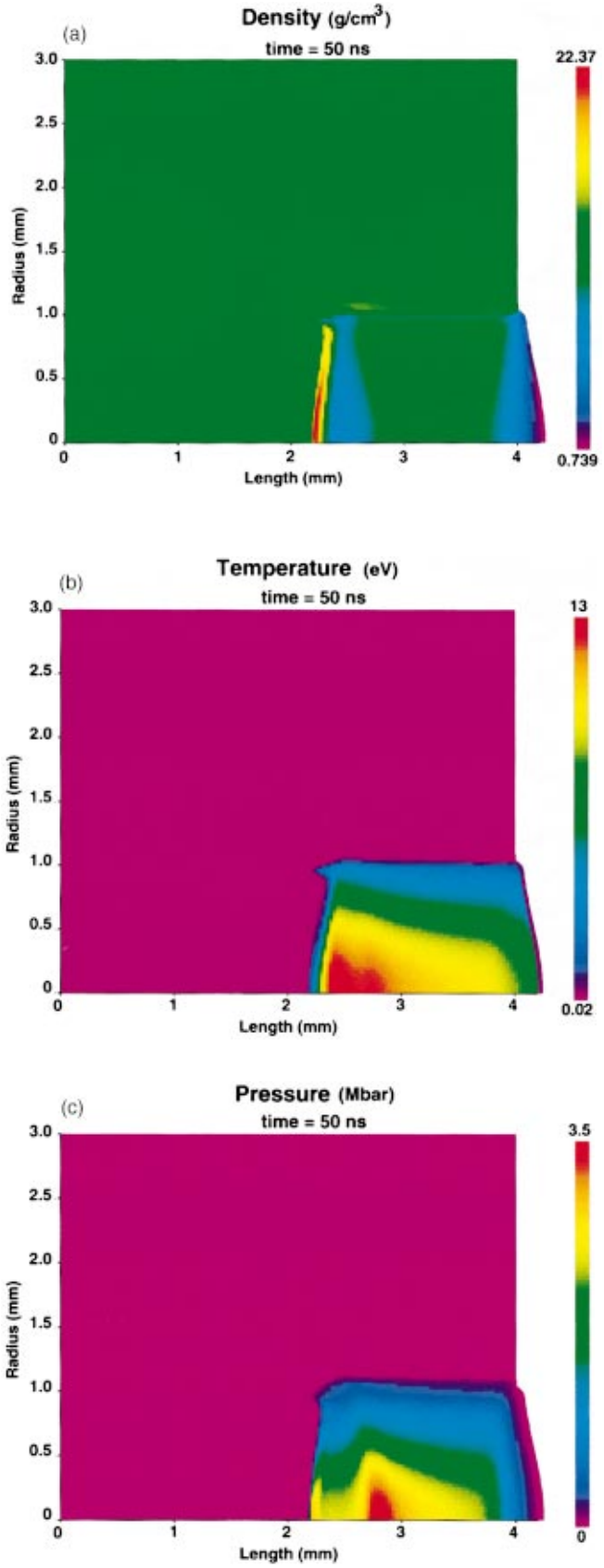

FIG. 3. (Color) (a) Density, (b) temperature, (c) pressure on a length-radius plane at $t=50$ ns for a solid lead cylindrical target, initial length 4 mm, initial radius 3 mm, irradiated by 2×10^{11} particles of uranium, particle energy 200 MeV/u, pulse duration 50 ns, parabolic power profile in time, Gaussian power deposition profile along the beam radius with a FWHM=1.0 mm.

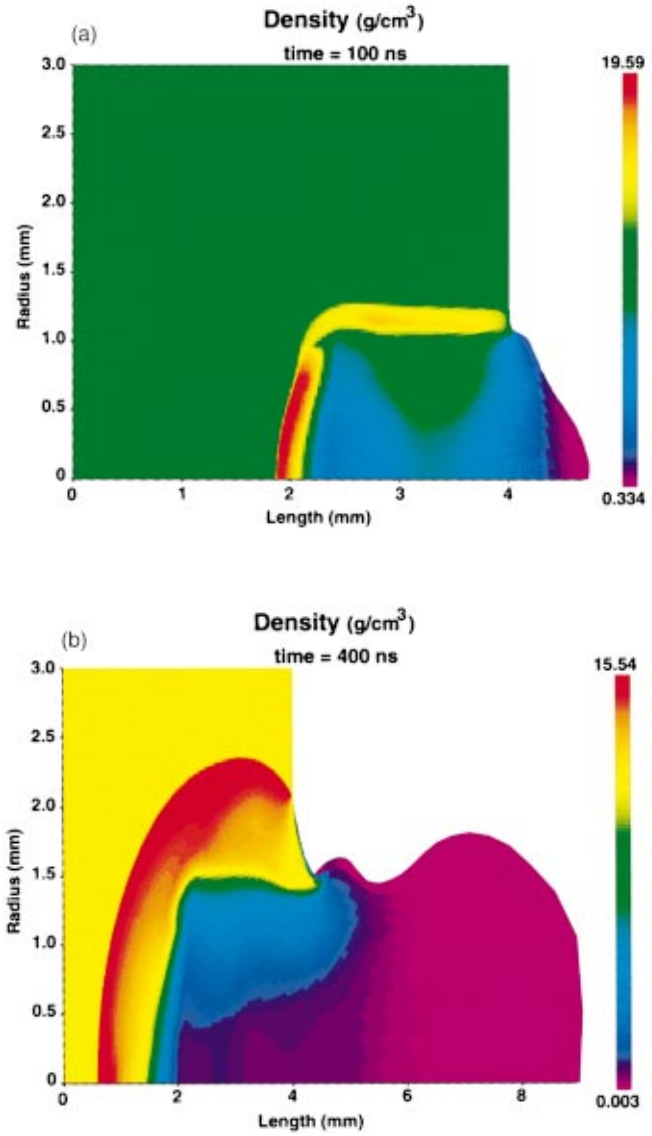

FIG. 4. (Color) (a) Same as in Fig. 3(a) but at $t=100$ ns, (b) same as in Fig. 3(a) but at $t=400$ ns.

of the Bragg peak, the density is still the solid-state density while the temperature is very high and the corresponding pressure is the highest (about 3.5 Mbar) and that creates the main pressure peak.

Figures 4(a) and 4(b) present the density as in Fig. 3(b), but at $t=100$ ns and 400 ns, respectively. Figure 4(a) shows that a two-dimensional shock wave has developed and because of the higher energy deposition in the Bragg peak and due to the Gaussian behavior of the energy deposition along the radius, the shock in the axial direction is much stronger than that in the radial direction. Material expansion from the beam-heated region is also shown in this figure.

Figure 4(b) shows that the shock has propagated outward, away from its original position and the shock strength has also been reduced due to the cylindrical nature of the shock wave.

These simulation results allow one to choose the diagnostic tools appropriate to the relevant parameter ranges. Since the shock wave in this experiment is not a planar stationary one, the diagnostics cannot be restricted to shock front and material velocity only but, rather, a complete set of diagnostic methods has to be employed. The surface velocities that appear in the experiment can be measured with streak or fast-framing cameras in shadowgraphy or by laser interferometry. The maximum surface temperature of about 10 eV corresponds to a maximum of the Planck radiation at a wavelength of about 30 nm, thus making pyrometry in the vuv region the method of choice by which to measure these temperatures. Measurement of the temperature inside the solid lead target, however, may not be an easy task. This difficulty may be overcome by using a target that contains fine holes that are drilled at suitable locations in that part of the target which is not directly irradiated by the ion beam. Pyrometric measurements through these fine holes could determine the shock front temperature at different locations inside the target at different times. One can also perform x-ray measurements in the same target arrangement. A comparison of the measured spectra with spectra that are simulated with a sophisticated atomic-physics–radiation model that includes a treatment for reabsorption could also provide detailed information about the temperature and the density of the material inside the target. Piezoelectric polymer stress gauges (PVDF) immersed in the solid lead target can be applied to measure pressures up to 0.1 Mbar as they appear in the outward-moving shock. The size of these gauges should be of the order of 1 mm$\times$1mm. Manganin pressure sensors are applicable in the 1-Mbar range in the center of the interaction region.

IV. CONCLUSIONS

This paper presents two-dimensional numerical simulations of the hydrodynamic response of a solid lead target that is irradiated by an intense heavy-ion beam that will be available at the GSI Darmstadt by the end of the year 2001, after the upgrade of the existing facilities, which will include introduction of a new, high-current injector and a powerful rf buncher, is completed. This upgraded facility will generate U^{28+} beams with a particle energy of 200 MeV/u that will be delivered in 50-ns-long pulses. Use of a multiturn injection scheme with intermediate electron cooling will allow acceleration of 2×10^{11} particles in the beam that translate to about 1.5 kJ total input energy. Our calculations show that strong shocks will be generated in the target and the maximum material density in the shock region could be about 22 g/cm^3, which is a factor of 2 higher than the solid lead density. The corresponding maximum pressure is about 3.5 mbar. This will allow, at the GSI the possibility of investigating the equation-of-state properties of high-energy-density matter.

ACKNOWLEDGMENT

We thank the BMBF for supporting this work.

[1] R. O. Bangerter, J. W.-K. Mark, and A. R. Thiessen, Phys. Lett. **88A**, 225 (1982).
[2] C. Deutsch and G. Maynard, Phys. Rev. A **26**, 665 (1982).
[3] C. Deutsch, Ann. Phys. (N.Y.) **11**, 1 (1986).
[4] T. Mehlhorn, J. Appl. Phys. **52**, 6522 (1981).
[5] E. Nardi and Z. Zinamon, Phys. Rev. Lett. **49**, 1251 (1982).
[6] N. A. Tahir and K. A. Long, Nucl. Fusion **23**, 887 (1982).
[7] G. R. Magelssen, Nucl. Fusion **24**, 1527 (1984).
[8] K. A. Long and N. A. Tahir, Phys. Rev. A **35**, 2631 (1987).
[9] D. H. H. Hoffmann, K. Weyrich, H. Wahl, D. Gardès, R. Bimbot, and C. Fleurier, Phys. Rev. A **42**, 2313 (1990).
[10] J. Jacoby, D. H. H. Hoffmann, W. Laux, R. W. Müller, H. Wahl, K. Weyrich, E. Boggash, B. Heimrich, C. Stöckl, H. Wetzler, and S. Miyamoto, Phys. Rev. Lett. **74**, 1550 (1995).
[11] H. Kitamura and S. Ichimaru, J. Phys. Soc. Jpn. **65**, 1250 (1996).
[12] A. V. Bushman and V. Fortov, Sov. Tech. Rev. B Therm. Phys. **1**, 219 (1987).
[13] R. Redmer, Phys. Rev. E **59**, 1073 (1999).
[14] E. Wigner and H. B. Huntigton, J. Chem. Phys. **3**, 764 (1935).
[15] S. T. Weir, A. C. Mitchell, and W. J. Nellis, Phys. Rev. Lett. **76**, 1860 (1996).
[16] H. K. Mao and R. J. Hemley, Rev. Mod. Phys. **66**, 671 (1994).
[17] N. A. Tahir, D. H. H. Hoffmann, J. A. Maruhn, K.-J. Lutz, and R. Bock, Phys. Lett. A **249**, 489 (1998).
[18] A. M. Evans *et al.*, Laser Part. Beams **14**, 113 (1996).
[19] B. Faral *et al.*, Phys. Fluids B **2**, 371 (1990).
[20] R. C. Cauble *et al.*, Phys. Plasmas **4**, 1857 (1997).
[21] R. W. Mueller and P. Spiller, GSI Report No. GSI-96-07, ISSN 0171-4546, 1998 (unpublished).
[22] P. Spiller and I. Hoffmann, Nucl. Instrum. Methods Phys. Res. A **415**, 384 (1998).
[23] N. A. Tahir, D. H. H. Hoffmann, J. A. Maruhn, K.-J. Lutz, and R. Bock, Phys. Plasmas **5**, 4426 (1998).
[24] N. A. Tahir, D. H. H. Hoffmann, J. A. Maruhn, P. Spiller, and R. Bock, Phys. Rev. E **60**, 4715 (1999).
[25] N. A. Tahir, K. A. Long, and E. W. Laing, J. Appl. Phys. **60**, 898 (1986).
[26] V. E. Fortov *et al.*, Nucl. Sci. Eng. **123**, 169 (1996).
[27] P. Spiller, GSI Report No. GSI-94-11, ISSN 0171-4546, 1994 (unpublished).
[28] M. Winkler, P. Spiller, B. Hartmann, C. Weil, H. Wolnik, W. Laux, H. Wahl, B. Heimrich, and D. H. H. Hoffmann, GSI 1991 Annual Report No. GSI-92-1, ISSN 0174-0814, 1992 (unpublished).
[29] P. Spiller, W. Laux, M. Dornik, H. Eickoff, H. Wolnik, M. Winkler, and D. H. H. Hoffmann, GSI 1994 Annual Report No. GSI-95-1, ISSN 0174-0814, 1995 (unpublished).
[30] M. Stetter *et al.*, Nuovo Cimento A **106A**, 1725 (1993).
[31] P. Spiller and I. Hoffmann, Nucl. Instrum. Methods Phys. Res. A **415**, 384 (1998).
[32] I. V. Lomonosov, A. V. Bushman, and V. E. Fortov, in *High-Pressure Science and Technology, 1993*: Proceedings of the Joint IARA/APS Conference, Colorado Springs, CO, 1993, edited by S. C. Schmidt, J. W. Schaner, G. A. Samara, and M. Ross, AIP Conf. Proc. No. **309** (AIP, New York, 1994), Part 1, p. 117.
[33] J. F. Ziegler, J. P. Biersack, and U. Littmark, *The Stopping and Ranges of Ions in Solids* (Pergamon, New York, 1996).